ISSN : 0974 - 7486 Volume 10 Issue 6

Materials Science

An Indian Journal

Full Paper

MSAIJ, 10(6), 2014 [205-212]

Synthesis and investigation of pillared layered / pyrrole

Mohamed Y.Abed[1], Dalia Elsawy[1], Nahla A.Mansour[1], Manal G.Mohamed[1]*, A.Ashary[2], Azza M.Mazrouaa[1]

[1]Petroleum Research Institute, Polymer laboratory, Petrochemical Department, Nasr City, Cairo, (EGYPT)

[2]Physics Department, National Research Center, Dokki, Cairo, (EGYPT)

E-mail : zinabmanal@yahoo.com

ABSTRACT

Polypyrrole was prepared by oxidation polymerization (polyaddition) of pyrrole with ratios of the oxidant (1:2), bentonite pillared nanocomposite clay based on Fe, Al, and Fe-Al was prepared. The polypyrrole nanocomposites was prepared and characterized via XRF, FTIR, XRD and TEM. The thermal stability and electrical conductivity of the polypyrrole and its nanocomposites were investigated. XRD and TEM proved that the particle size of Bentonite was reduced when exfoliated in the polypyrrole. It was found that the thermal stability and electrical conductivity of the PPy were enhanced by the addition of metal-pillared Bentonite. It was found the I-V relation is Ohmic, and the conduction mechanism of the reaction is electronic.

KEYWORDS

Polypyrrole;
Pillared clay;
Nanocomposites;
Electrical conductivity and thermal stability.

INTRODUCTION

Amongst the conducting polymers, polypyrrole is one of the most frequently studied polymers, having high electrical conductivity, ion exchange property, environmental stability, non toxicity, and low cost. More efforts have been made to synthesize polypyrrole nanocomposites for a myriad of applications. Conducting polymer/inorganic clay nanocomposites provide the new synergistic properties, which cannot be attained from individual materials, such that the conductivity is more easily controlled, and the mechanical or thermal stability is improved through the synthesis of the nanocomposites[1]. Abdul Shakoor et.al recently reported preparation, characterization and electrical conductivities of polypyrrole/aluminum pillared montmorillonite (PPy/Al_PMMT) clay nanocomposites[2]. Apart from the general tailor, ability of their chemical and physical properties these composites showed enhanced AC and DC conductivities as compared to pristine PPy[2], which make these composites interesting materials for device applications.

Hong et al.[3] synthesized polypyrrole –montmorillonite nanocomposites for application in electronic devices such as light emitting diodes and as corrosion resistant, Hosseini et al.[4], studied the effect of polypyrrole–montmorillonite nanocomposites powder addition on corrosion performance of epoxy coatings on Al 5000, while Bae et al.[5] synthesized a fully exfoliated nanocomposite from polypyrrole graft copoly-

Full Paper

mer /clay for potential applications in many ûelds such as optics, ionics, electronics, and mechanics. Because of their ion exchange property, PPy and its modiûed materials are important adsorbents for removing pollutants from water waste[6].

The polymerization of pyrrole (PY) in aqueous or alcohol/water mixed medium in presence of $FeCl_3$ and nanodimensional Al_2O_3 resulted in the formation of conducting nanocomposites of polypyrrole (PPY)/Al_2O_3[7]. In this work, $NaClO_4$ in water either $HClO_4$ or HCl polymerized pyrrole were precooled and added in order to ensure acidic medium. In addition, $HClO_4$ is a co catalyst because it supplies the medium with ClO_4ions, and prepared nanocomposites bentonite clay based Fe, Fe-Al and Al pillared bentonite clay and tested their electrical conductivity and thermal stability. The aim of the present research was the improvement of the electrical and thermal properties of polypyrrole by adding pillared bentonite.

EXPERIMENTAL

Materials

Pyrrole was obtained from BDH, it was distilled under vacuum. Sodium perchlorate $NaClO_4$ and perchloric acid $HClO_4$ was obtained from Aldrich. $NaClO_4$ was recrystallized from ether, HClO4 from was used as it is. Bentonite clay was obtained from Aldrich. The cation exchange capacity of the bentonite was determined to be 1.15 meq.g-1.Fe $(NO_3)_3$ from Sigma were used directly without further purification.

Synthesis of polypyrrole[8-10]

1 mol pyrrole (67 gm =69.2ml) is added to 2 mole of sodium perchlorate (225 gm), the molar ratio of pyrrole: sodium perchlorate was 1:2 and 100 ml precooled perchloric acid $HClO_4$at 0°C. The mixture was maintained in ice at 0oC, for 10 minutes. Polypyrrole was separated by filtration, washed with precooled water and methyl alcohol, and dried in air under vacuum desiccators.

Synthesis of pillared layered Fe_2O_3- Bentonite[11,12]

A solution of 0.2M ferric nitrate was prepared by dissolving the equivalent amount of the salt in deionized and distilled water. Solid sodium carbonate was added slowly to alter the pH of the solution, hydrolysis of ferric nitrate with sodium carbonate was carried out at 25°C, and an aging period of 24 h was allowed. The value of OH/Fe was 2.0 and the pH of this solution was 1.8. A suspension containing 1.0 g of bentonite clay in 100 ml water was added to the hydrolyzed ferric solution. This suspension and the pillaring agent were vigorously stirred at room temperature for 24 hr, recovered by filtration, washed repeatedly with water, and then dried in air over night at 110°C. The filtrate was calcined at 300°C for 5h.

Synthesis of pillared layered Al_2O_3 and Fe-Al Bentonite[11,12]

The same procedure was made as in Fe_2O_3 -Bentonite.

Preparation of pillared Layered /Polypyrrole nanocomposites

85 wt % of polypyrrole were mixed with 15 wt% of prepared pillared layered Fe_2O_3-bentonite, Al_2O_3-bentonite and Fe-Al- in hot mixer. In the melt intercalation, pillared layered are directly mixed with the polymers matrix in the molten state. Then the powder of pillared layered/ppy was sieved at 0.16 mm.

Characterization

- The atomic absorption: the bentonite and pillared bentonite were measured in the micro analytical center in Faculty of Science-Cairo University as shown in [TABLE1].
- IR spectra : recorded on Jusco FTIR 300E Fourier transform infrared spectrometer (Tokyo, Japan).
- X-ray diffractometer : used to characterize the structure of the samples by using Diano computer controlled (formally made by Diano Corporation, USA). The target was cobalt energized by 45Kv/ 10mA and graphite monochromator. The counter was sintellation with dead time 10^{-6}sec.
- TEM Micrograph: JEOL JEM-1230 Electron Microscope measured the polypyrrole-clay.
- A Shimadzu TGA: 50 systems in a nitrogen atmosphere (30 mL/min) were used. The temperature range was from the ambient temperature to 600°C. The rate of heating rate is 10°C/min.
- The electric circuit: consists of an electric source,

the cell, high impedance electrometer (A. Kiethley electrometer of the type 610 C of sensitivity 10^{-14} ampere) and a variable resistance. A sample of the polymer and the polymer complex was pressed into 1 mm thickness in a special vacuum mold the pressure was 3770 Kg/cm^2.

RESULTS AND DISCUSSION

Characterization of metal-bentonite nanocomposites

Chemical composition

[TABLE 1] gives the elemental analyses of the prepared pillared clay, determined by XRF. During the pillaring of the bentonite clay with Fe_2O_3, analysis shows that 28.6% Fe has contributed to the constitution of the pillars. However, in Fe-Al-PILC, only 7.2% Fe has additionally contributed to the constitution of pillars. On the other hand, Al, participation in the pillars = 23.2 - 18.7= 4.5 %, since bentonite originally contained 18.7% of aluminum. However, aluminum in the Fe-Al-PILC comprises 9.4%.

TABLE 1 : XRF data for the prepared pillared clay

Sample	Na	Fe	Si	Al
Bentonite	1.69	5.4	69.3	18.7
Fe- PILC	0	34.0	51.5	14.5
AL- PILC	0	9.2	63.4	23.2
Fe-Al- PILC	0	12.6	50.6	28.2

Specific surface area

The specific surface area of the bentonite clay is 28.4 m^2g^{-1}, where as those of the prepared Fe-PILC and Fe-Al-PILC were 280 and 245 m^2g^{-1}, respectively. Evidently, the combined Al-Fe pillaring has decreased the surface area than that of the Fe-PILC [TABLE 2].

TABLE 2 : Physico-chemical characteristics of prepared catalyst

Sample	Surface area m^2 g^{-1}	Particle size, nm Form XRD
Fe-PILC	280	12.2
Fe-Al-PILC	245	9.9

XRD

The XRD pattern of the host clay shows diffraction peaks at 2θ = 26.6 and 19.88, which are assigned to SiO_2 crystallite[13]. For Fe-PILC, the main diffraction peaks are at 2θ = 33.2 and 35.5, assigned to Fe_2O_3 crystals. The XRD data indicated that Fe particles are intercalated in silicate layers in the catalysts. The size particles calculated from these data for the current catalysts are listed in [TABLE 2].

FTIR

The FTIR spectra of the raw Na^+-bentonite and the prepared pillared bentonite samples in the region 2000-500 cm^{-1} are illustrated in Figure.1 (a-d). Sharp bands (Figure. 1a) at 523 and 456 cm^{-1} attributed to the vibration of the Si-O group and Si-O-Al groups due to kaolinite. The bands at 722 and 621 cm^{-1} correspond to the isolated AlO_4 tetrahedra and alternating SiO_4 and AlO_4 tetrahedra, respectively[14]. The band centered at 910cm^{-1} related to the Al-OH group. The large and relatively broad band at 1044 cm^1 is characteristic of bentonite. The 1625 cm^{-1} is characteristic of pseudo layer silicates, interstratified minerals. This bentonite structure is still present in the FTIR spectra obtained for the Al-PILC (Figure.1b), Fe-PILC (Figure.1c) and Fe-Al-PILC (Figure.1d) after carrying out the pillaring process.

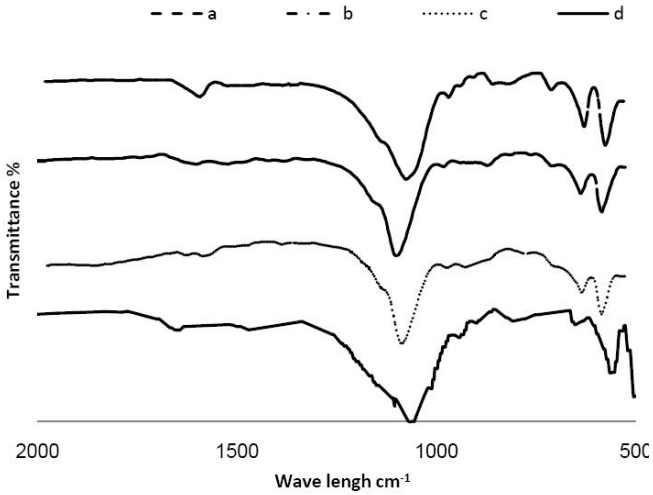

Figure 1 : FTIR of the prepared pillared / bentonite

Transmission electron microscope of the pillared bentonite

TEM of the original bentonite clay shows a plain view with some few lamellar features lightly distributed all over the slide (Figure 2a). TEM of Fe-PILC shows multiple walls, which may be in accordance with the

Full Paper

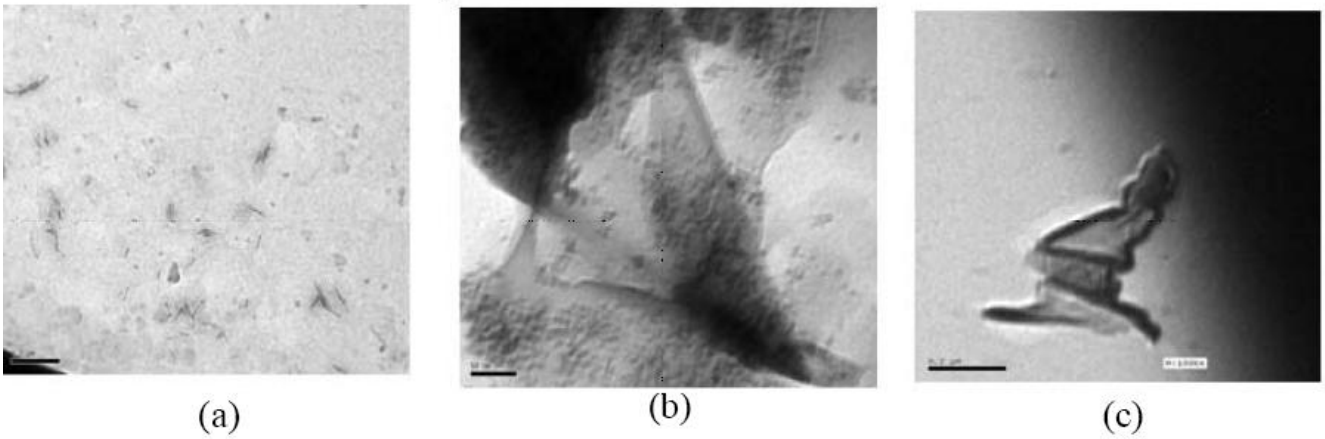

Figure 2 : TEM image of the pillared bentonite

high percentage of Fe in this PILC. The pillars exhibit various crystalline planes with separate shadings. The photograph shows also a large pyramidal wall (Figure 2b).

However, the TEM of Fe-Al-PILC (Figure 2c) may reveal a distinct pillar, which appears to be constructed of more than one segment. The lower basal segment seems to be horizontally laying on the bentonite landscape. The second segment is a rectangular part, which may be a well developed crystal. The dark color of this part implies that it may be composed of Fe or Fe_2O_3.

nalytical Measurements of polymer nanocomposites:

FTIR

The peaks at 1298 cm^{-1}, 1652 cm^{-1}, 1560 cm^{-1} and 3000 cm^{-1} are due to C-N, C=N, C=C and C-H aromatic vibration respectively of polypyrrole and the peaks at 527 cm^{-1} and 310 cm^{-1} are due to the presence of SiO_4 and $Al(OH)_4$ which indicates that the Na^+-bentonite was reacted with the PPy[15]. The characteristic vibrations of Na^+-MMT is known to be in the region of 700 cm^{-1} to 1700 cm^{-1}[16]. The bands of Na^+-MMT are observed at 1637 cm^{-1} (H-O-H bending of water molecule), 1040 cm^{-1} (Si-O stretching), 918 cm^{-1} and 795 cm^{-1} (Al-O bending)[17,18].

The band at 1296 cm^{-1} in the spectrum of a mechanical mixture of PPy and MMT is shifted to 1311 cm^{-1} in the spectra of the intercalated nanocomposites. This shift is due to the physicochemical interaction (hydrogen bonding between –NH group of PPy and –O of silicate) in the intercalated PPy-MMT[16,19] whereas mechanical mixtures of PPy and MMT lack such an interaction. The absorption bands at 1032, 310, 372 and 467 cm^{-1} belong to Si–O–Si, $Al–(OH)_4$, $Si–(O)_2$ and Si–O–Fe vibrations, respectively.

X-Ray diffraction (2è)

The XRD patterns of PPY/Pillared layered nanocomposites with the different pillared layered Bentonite are shown in Figure (3). The diffraction peak of pillared-Bentonite is almost invisible in the patterns for PPY+ Fe- Bentonite and PPY+ Al- Bentonite and weak for PPY+ Fe-Al- Bentonite (d= 1.4). This result suggested that the layered silicate galleries of the PPY+ Fe-Bentonite and PPY+ Al- Bentonite have been either intercalated to a space of more than 3.5 nm (2θ < 2æ%) or exfoliated in the PPY[20]. This will be confirmed by TEM images, where it is well known that, while XRD analysis gives the macroscopic conformation of a sample, TEM photograph shows the local microscopic conformation.

Transmission electron microscopy (TEM):

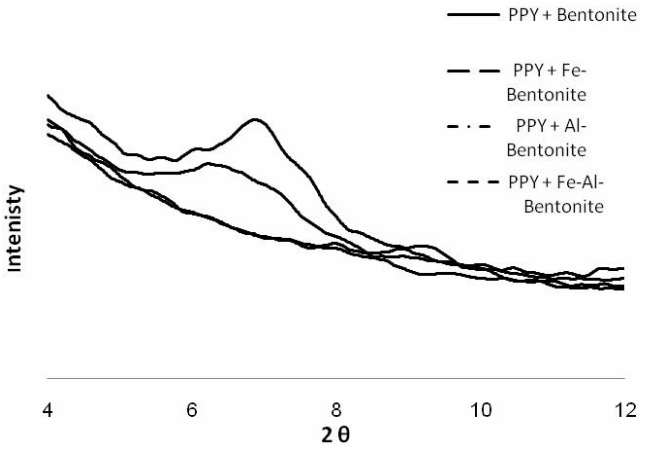

Figure 3 : XRD of PPY- Pillared nanocomposites.

The morphology of the unmodified bentonite and PPY/Pillared layered nanocomposites is shown in Figure (4). The Figure shows the morphology of the bentonite which intercalated or exfoliated in the polypyrrole and confirms the trends in dispersion that were suggested by the XRD data. The TEM images show that the dispersion of metal-clay is much better and tend to nanostructure than the polypyrrole. In this morphological, the ultrafine inorganic oxide particles are not only present on the surface, but are also distributed throughout the interior of the agglomerates[20]. From the TEM, we can observe that the size of the bentonite was modified and the particle size of it was reduced to 16 nm

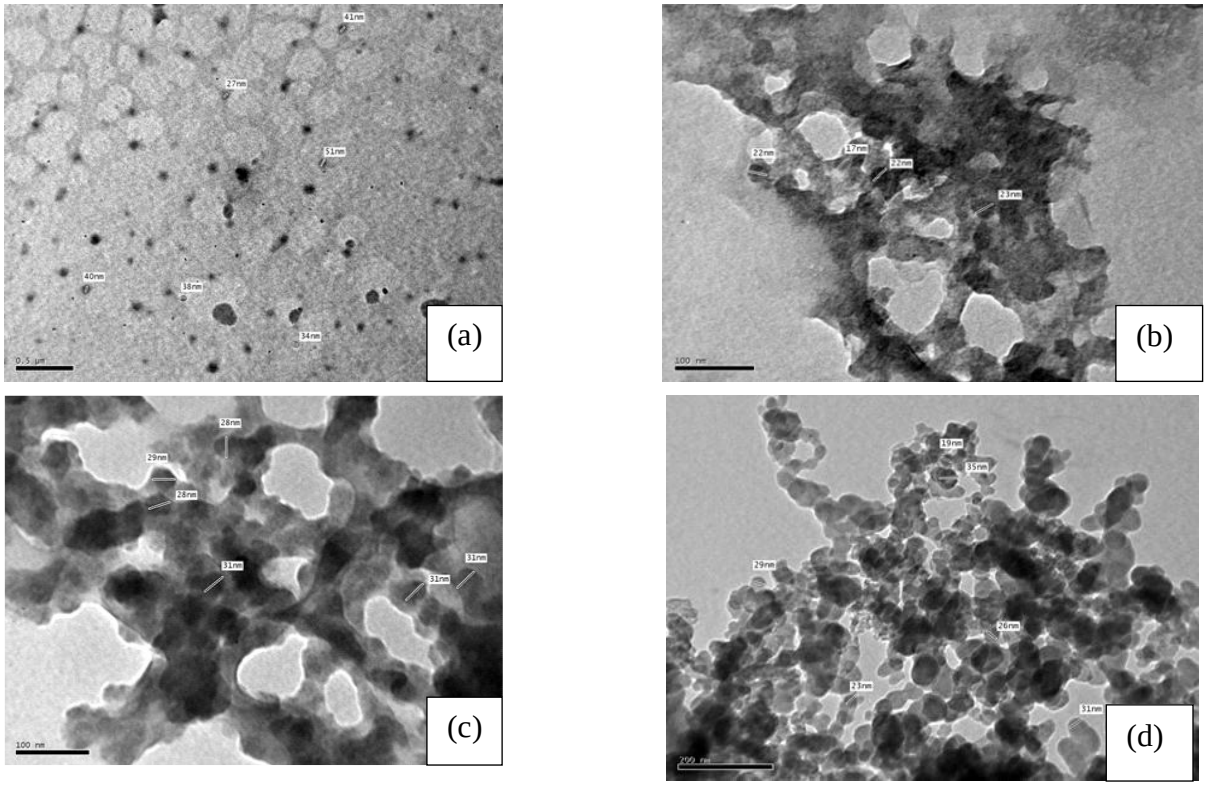

Figure 4 : TEM image of PPy+ Na-Bentoite (a), PPy+ Fe- Bentonite (b), PPy + Al-Bentonite (c) and PPy + F-Al- Bentonite (d).

when exfoliated in polypyrrole.

Thermogravimetric analysis (TGA):

The thermal stability of polymeric materials is usually studied by thermo-gravimetric analysis (TGA). The weight loss due to the formation of volatile products after degradation at high temperature is monitored as a function of temperature. When the heating occurs under an inert gas flow, a non-oxidative degradation occurs, while the use of air or oxygen allows oxidative degradation of the samples. Generally, the incorporation of clay into the polymer matrix was found to enhance thermal stability[22]. However, thermal behavior of polymer/clay nanocomposites is complicated and many factors contribute to increase in thermal resistance. Due to characteristic structure of layers in polymer matrix and nanoscopic dimensions of filler particles, several effects have been observed that can explain the changes in thermal properties.

The TGA thermograms of the PPY/pillared bentonite nanocomposites and pure sample of PPY are shown in Figure (5). It can be seen that with addition of the pillared bentonite, the thermal stability of the PPy film was significantly increased. As listed in TABLE (3), $T_{5\%,}$ the temperatures at which 5% weight-loss of the PPy/pillared bentonite nanocomposites occurred, are 7, 11 and 15 æ%C higher than that of the pure PPy for PPy + B-Fe PPy + B-Al, PPy + B-Fe-Al. The values of $T_{50\%}$, the temperatures at which the 50% weight-loss occurred for all PPy/pillared bentonite nanocomposites are higher than that of pure PPy by 15, 91, 82 °C for PPy + B-Fe PPy + B-Al, PPy + B-Fe-Al. These results confirm that the thermal stability of the PPy/pillared

Full Paper

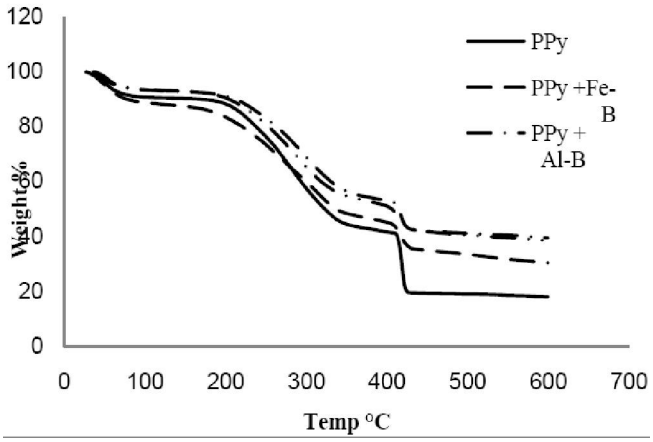

Figure 5 : TGA of the PPY nanocomposites

TABLE 3 : Thermal parameters of PPy and PPy/Pillared Bentonite

	$T_{5\,\%}$ °C	$T_{50\%}$ °C	char residue (wt% at 500 °C)
Pure PPy	53.96	322.7	19.13
PPy + B-Fe	60.71	337	33.57
PPy + B-Al	64.15	414	41.19
PPy + B-Fe-Al	68.3	405	40.56

bentonite nanocomposites was enhanced due to the presence of the metal bentonite. The increase in thermal stability could be attributed to the high thermal stability of bentonite and the interaction between the bentonite particles and the polymer matrix[23].

The introduction of inorganic components into organic materials can enhance their thermal resistance, as the dispersed silicate layers hinder the permeability of volatile degradation products out of the material and assist the formation of char after thermal decomposition[23]. Besides, the char yield at 500 æ%C for nanocomposite series was also increased as expected than the pure PPy.

Electrical conductivity:

Conducting polymers are amorphous with short conjugation lengths. Therefore, it has been suggested that electrical conduction takes place by charge hopping between polymeric chains. When the electric field is applied to conducting polymers, it assumes that electron transport originates from localized or fixed states within the polymer chain. The charge transfer between the chains takes place by hopping, referred to as phonon assisted hopping, between two localized states[17]. Most of the curves between the current I and the voltage V

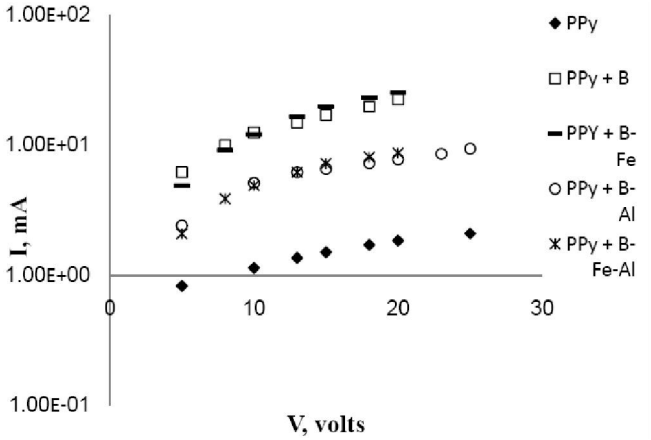

Figure 6 : I&V Charecterization of PPy and PPy Pillared Bentonite nanocomposites

are linear passing through the origin. This means that the relation is Ohmic and that the mechanism of the reaction is electronic as shown in Figure (6).

The increment in temperature provides an increase in free volume and segmental mobility[24]. These two entities then permits free charges to hop from one site to another thus increase conductivity. The conductivity increases so as temperature indicates more ions gained kinetic energy via thermally activated hopping of charge carriers between trapped sites, which is temperature dependence. The sharp increase of dc conductivity between 333 K to 358 K can be attributed to large heat energy absorbed by the samples and thus induce mobility of electrons[25]. It is suggested that in the region, the band gap between valence band and conduction band is reduce significantly and provide easiness for electrons to hopping from valence band to conduction band and hence gives higher dc conductivity val-

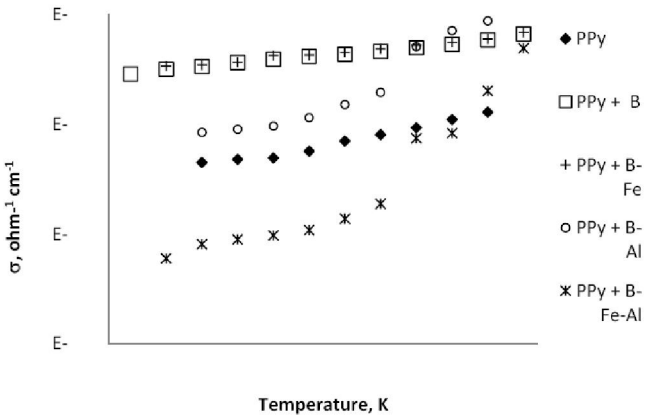

Figure 7 : The temperaure dependence of dc. conductivity of PPy and PPy Pillared Bentonite nanocomposites

ues as compared to other temperatures[24]. The relation between log σvs. T in most cases appear to be similar to that in semiconductors as shown in Figure (7).

The specific electric conductivity increases up to 1x 10^{-1}&!$^{-1}$.cm^{-1} which is in the range of semiconductors.

There are two major preliminary conclusions that could be drawn from Figure (8) which shows the electrical conductivity of PPy Pillared Bentonite

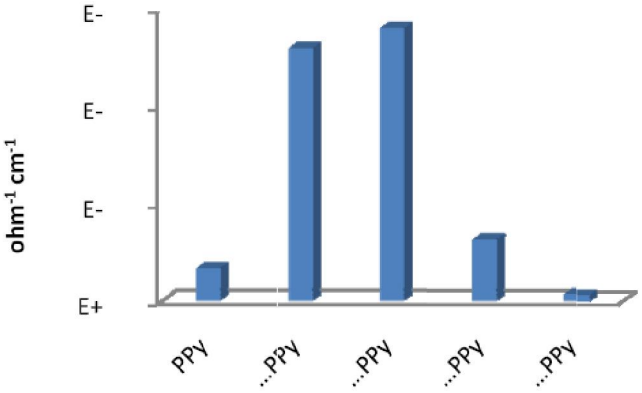

Figure 8 : the electrical conductivity of PPy Pillared Bentonite nanocomposites at 50 °C

nanocomposites at 50 °C:

(i) the electrical conductivity of PPy+B-Fe ~ PPy + B Ã PPy + B-Al> PPy > PPy + B -Al-Fe.

(ii) the metal Pillared bentonite effective in producing clay/polypyrrole nanocomposites with an enhancement of conductivity by about 2–3 orders of magnitude compared to the pure PPy. This increase in conductivity is attributed to the intercalation of polypyrrole chains in the interlamellar galleries of the pillared clay[26].

The activation energy (E_a) value for PPy/Pillared Bentonite nanocomposites and PPy –Bentonite is less than that of pure PPy, which indicate that the process of conduction becomes easier TABLE (4). These values of E_a are close to the value of E_a in[21,27]. The final look of the table shows that the second activation energy region E_2 is almost higher than that of the first region E_1. This is due to the higher dissociation energy needed to form the charge carriers for the intrinsic conduction[28].

TABLE 4 : The activation energy of the dc conductivity in low (E_1) and high (E_2) temperature regions respectively for PPy Pillared Bentonite nanocomposites.

	ΔE_1, eV	ΔE_2, eV
Pure PPy	0.83	1.43
PPy + B	0.52	0.87
PPy + B-Fe	0.49	0.79
PPy + B-Al	0.75	2.45
PPy + B-Fe-Al	1.03	3.38

CONCLUSION

Polypyrrole was prepared by oxidation (polyaddition) of pyrrole with ratio of the oxidant (1:2). Bentonite pillared nanocomposite clay based on Fe, Al and Fe-Al was prepared. The XRD and TEM observed that the size of the bentonite was modified and the particle size of it was reduced to 16 nm when exfoliated in polypyrrole. The thermal stability of the PPy/Pillared Bentonite nanocomposites was increased than pure PPy due to the presence of the metal Bentonite. The current I and the voltage V relation was Ohmic and the reaction mechanism was electronic. The specific electric conductivity increases up to 1x 10^{-1}&!$^{-1}$.cm^{-1} which is in the range of semiconductors. The metal Pillared bentonite effective in producing clay/polypyrrole nanocomposites with an enhancement of conductivity by about 2–3 orders of magnitude compared to the pure PPy. The activation energy (E_a) value for PPy/Pillared Bentonite nanocomposites and PPy –Bentonite is less than that of pure PPy,

ACKNOWLEDGEMENTS

The authors gratefully acknowledge Prof. Dr.Sahar Mostafa, Professor in Petro chemical Department, Petroleum Research Institute.

REFERENCES

[1] J.W.Kim, F.Liu, H.J.Choi, S.H.Hong, J.Joo; Polymer, **44**, 289 **(2003)**.

[2] A.Shakoor, H.Anwar, T.Z.Rizvi; J.Compos.Mater., **42**, 2101 **(2008)**.

[3] S.H.Hong, B.H.Kim, J.Joo, J.W.Kim, H.J.Choi; Curr.Appl.Phys., **1**, 447–450 **(2001)**.

[4] M.G.Hosseini, M.Raghibi-Boroujeni, I.Ahadzadeh, R.Najjar, M.S.Seyed Dorraji; Prog.Org.Coat., **66**, 321–327 **(2009)**.

[5] W.J.Bae, K.H.Kim, W.H.Jo, Y.H.Park; Polymer,

46, 10085–10091 **(2005)**.
[6] K.Z.Setshedi, M.Bhaumik, S.Songwane, M.S.Onyango, A.Maity; Chemical Engineering Journal, **222**, 186–197 **(2013)**.
[7] S.S.Ray; Materials Research Bulletin, **37(5)**, 813-824 **(2002)**.
[8] Y.Fu, R.A.Weiss, P.P.Gan, M.D.Besette; Polym.Eng.Sci., **38**, 857 **(1998)**.
[9] E.J.Oh, K.S.Jang, A.G.MacDioumid; Synth.Met., **125**, 267 **(2002)**.
[10] M.Omastova, M.Trchova, J.Kovarova, J.Stejskal; Synth.Met., **138**, 447 **(2003)**.
[11] E.G.Rightor, M.S.Tzou, T.J.Pinnavaia; J.Catal., **130**, 29 **(1991)**.
[12] H.J.Choe, I.S.Nam, S.W.Ham, S.B.Hany; Catal.Today, **68**, 31 **(2001)**.
[13] G.Chen, S.Liu, S.Chen, Z.Qi; Macromol.Rapid Commun., **21**, 746 **(2000)**.
[14] D.Lee, K.Char, S.W.Lee, Y.Park; J.Mater.Chem., **13**, 2942 **(2003)**.
[15] W.M.De Azevedo, M.O.E.Schwartz1, G.C.do Nascimento, E.F.J.da Silva; Phys.Stat.Sol.(C), **1** S249 **(2004)**.
[16] J.K.Mishraa, J.Ryoub, G.Kimc, K.Hwanga, Il Kima, Ch.Haa; Materials Letters, **58**, 3481–3485 **(2004)**.
[17] Tr.Akif Kaynak; J.of Chemistry, **22**, 81-85 **(1998)**.
[18] Encyclopedia of Science and Technology, McGraw-Hill 9th Edition, **(2002)**.
[19] Y.Tominaga, S.Asai, M.Sumita, S.Panero, B.Scrosati; Power Source, **146**, 402-406 **(2005)**.
[20] J.M Yeh, S.J Liou, M.C Lai, Y.W Chang, C.Y Huang, C.P Chen; J.Appl Polym Sci., **94**,1936–46 **(2004)**.
[21] S.G Shangbin, Z.Jifu, W.Qiumei, L.Yugeng; Electrochimica Acta, **52**, 7315–7321 **(2007)**.
[22] A.Leszczy´nska, J.Njuguna, K.Pielichowski, J.R.Banerjee; Thermochimica Acta **454**, 1–22 **(2007)**.
[23] S.Sankaraiah, C.Sung-Wook, L.Jun-Young, K.Jung-Hyun; Polymer, **48**, 4691-4703 **(2007)**.
[24] H.Mohd, S.Elias, K.Anuar, Y.H.Muhd, S.M.Iskandar, A.A.O.Muhd; Malaysian Polymer Jounal (MPJ), **3(2)**, 24-31**(2008)**.
[25] M.Batzill *; Ulrike Diebold The surface and materials science of tin oxide Progress in Surface Science, **79**, 47–154 **(2005)**.
[26] A.Shakoora, T.Z.Rizvib, M.Saeeda; COMPOSITES, **54(5)**, 401–406 **(2012)**.
[27] C.C.Yang; Mater.Sci.Eng.B, **131**, 256 **(2006)**.
[28] H.Adachi, Y.Ichikawa, K.Setsune, S.Hatta, K.Hirochi, K.Wasa; J.Appl.Phys., **27(4)**, L643 **(1988)**.